ACTIVE CONTROL LAW DESIIGN FOR SUPPRESSION OF FLUTTER AND GUST RESPONSE OF AEROELASTIC PANEL VIA SEGMENTED PIEZOELECTRIC ACTUATORS

S. A. Fazelzadeh & S.M. Jafari
Mechanical Engineering Department, Shiraz University, Shiraz, I.R. Iran

ABSTRACT

The purpose of this paper is to present an active control law for suppression of flutter and gust response of a rectangular panel using segmented piezoelectric actuators. Classical laminate theory with induced strain actuation and a generalized form of Hamilton's principle are used to formulate the governing equations of motion. The aerodynamic modeling is accomplished by first order piston theory with gust velocity effects. By using Rayleigh-Ritz method, the results equation for square and cross piezoelectric configurations are developed. Using an optimal integral control model as a part of linear quadratic regulator feedback loop together with a feedforward of the disturbances, greatly enhance the transient response and the steady state error characteristics of this system is observed. Furthermore, the numerical results for the passive and active panel are validated with the published results and excellent agreement is satisfied.

1. INTRODUCTION

Smart structure technology has found a wide range of applications in the fields of active vibration control, noise reduction and adaptive shape control. A number of materials such as piezoelectric, shape memory alloys, electro-reological fluids and optical fibers have adaptable properties, so that they can be used as actuators and/or sensors in smart structure applications.

In recent years, piezoelectric materials such as actuator/sensor have been widely used in aerospace industry partly due to their inherent properties to reduce undesired vibrations and flutter suppression. The possibilities of employing adaptive materials to control panel flutter investigated by Scott and Weisshaar (1994). They used linear quadratic regulator feedback control method. Development of the aerelectroelastic model consists of combining the electroelastic panel model developed by Hagood et al (1990) with the aeroelastic panel model introduced by Frampton et al (1996). They investigated the active control of panel flutter with piezoelectric transducers by using direct rate feedback control (DRFC) scheme.A review of the state of the art of smart structures was performed by Chopra (2002). A review about the active structural vibration control is presented by Alkhatib and Golnaraghi (2003). Ghanbarpoor et al (2004) used piezoelectric laminated actuators for wing structure that can adapt to gust condition. They developed a LQG control system for flutter suppression cantilevered supersonic panel under vertical random gust excitation. Abdel-Motagaly et al (2005) developed simulation models for a particular problem of vibration control: that of non-linear panel flutter suppression. Han et al (2006) presented a numerical and experimental investigation on active flutter suppression of a sweptback cantilevered lifting surface using piezoelectric actuation. Sebastijanovic et al (2007) used a basic eigenvector orientation approach to evaluate the possibility of controlling the onset of panel flutter using a simple flat panel.

This paper presents an active optimal control for supersonic panel flutter suppression and gust alleviation for two segmented piezoelectric arrangements. The aerodynamic modeling is accomplished by first order piston theory. Through the addition of the disturbance vectors to the dynamical equations, various atmospheric conditions are simulated. Parametric studies for three configurations piezoelectric actuator are considered. The optimal control problem is set up to minimize panel deflection using linear quadratic regulator (LQR). Using an integral control model as a part of feedback loop together with a feedforward of the disturbances is shown to greatly enhance the transient response and the steady state error characteristics of this system.

2. THEORY

2.1 Basic equations

An electroelastic panel with a length a, width b is considered. figure 1 shows the three-dimensional panel model, with simply supported conditions, deformed under the effect of external fluid flow passing over the panel top surface. The in-plane displacements are assumed negligible as compared to the panel transverse deflection (Frampton et al,

1996).

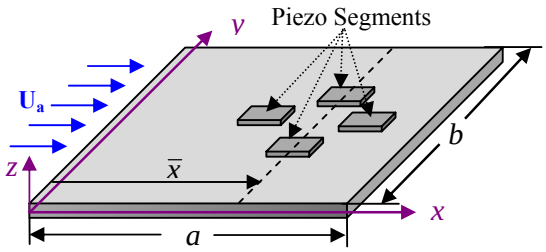

Figure 1: *Aerelectroelastic panel coordinate system*

To derive the governing equation of motion for aeroelastic piezo-panel, in supersonic flow with piezo-electrically coupled electromechanical properties, we use the generalized form of Hamilton's principle

$$\int_{t_1}^{t_2}\left[\delta(T-U+W_e)+\delta W_{nc}\right]dt=0 \tag{1}$$

where T is the kinetic energy, U is the potential energy, W_e is the electrical energy and W_{nc} represent non-conservative works (Hagood et al, 1990). The total kinetic energy of the system is

$$T=\int\frac{1}{2}\rho_s\,\dot{w}^2dV_s+\int\frac{1}{2}\rho_p\,\dot{w}^2dV_p \tag{2}$$

where w is the panel transverse deflection, ρ is mass density and V is the volume integral. Subscripts s and p are related to structure and piezoelectric, respectively. The potential energy of the system can be written as

$$U=\int\frac{1}{2}\mathbf{S}^T\mathbf{T}dV_s+\int\frac{1}{2}\mathbf{S}^T\mathbf{T}dV_p \tag{3}$$

where $\mathbf{S}$ is the vector of material strains and $\mathbf{T}$ is the vector of material stresses. Also the electrical energy of the system can be written as

$$W_e=\int\frac{1}{2}\mathbf{E}^T\mathbf{D}\,dV_p \tag{4}$$

where $\mathbf{E}$ is the electric field vector and $\mathbf{D}$ is the electric displacement vector. The virtual work due to the aerodynamic pressure is of the form

$$W_{nc}=\int p\,w\,dA_s \tag{5}$$

where p is the aerodynamic pressure and A_s is the surface integral. The aeroelastic pressure loading with gust effects (Ghanbarpoor asl et al, 2004) on the panel determined using piston theory is

$$p(x,y,t)=\frac{\rho_a U_a^2}{M_\infty}\left[\frac{\partial w}{\partial x}+\frac{1}{U_a}\left(\frac{\partial w}{\partial t}+W_G\right)\right] \tag{6}$$

where M_∞ is free stream Mach number, ρ_a is the free stream density and U_a is the free stream velocity and W_G is the vertical velocity component of random gust velocity. The random gust is supposed to be of a white noise character.

2.2 Rayleigh-Ritz formulation

The Rayleigh-Ritz formulation is employed for approximating generalized forces to discretize the coupled equations of motion (Scott and Weisshar, 1994). Schematic Piezo actuator placement is shown in figure 2.

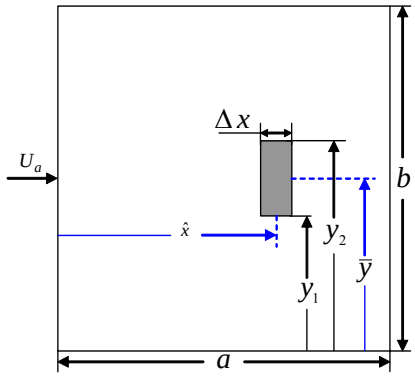

Figure 2: *Piezo actuator placement*

The out of plane deformation w is defined in physical coordinates as a series expansion of weighted summation of orthogonal modes over the generalized coordinates as

$$w(x,y,t)=\sum_{n=1}^{N}\psi_n(x,y)q_n(t)=\mathbf{\Psi}(\mathbf{x})\cdot\mathbf{q}(t) \tag{7}$$

where q_n is the generalized coordinates for the nth mode, and for simply supported panel, mode shapes ψ_n are sine function of the form

$$\psi_n(x,y)=Sin(n\pi\,x/a)\,Sin(\pi\,y/b) \tag{8}$$

By introducing non-dimensional parameter, the panel equation can be expressed non-dimensionally as

$$\begin{aligned}&(\hat{\mathbf{M}}_s+4\mu_p\hat{\mathbf{M}}_p)\ddot{\mathbf{r}}+\frac{1}{4M_\infty}\hat{\mathbf{D}}\dot{\mathbf{r}}\\&+\left(\frac{\mu_a}{\lambda}\hat{\mathbf{K}}_s+4\frac{\mu_a\sigma}{\lambda}\hat{\mathbf{K}}_p+\frac{1}{M_\infty}\hat{\mathbf{L}}\right)\mathbf{r}\\&=8\frac{\mu_a\sigma\varepsilon}{\lambda}\hat{\mathbf{\Theta}}\hat{\mathbf{v}}-\frac{1}{4M_\infty}\hat{\mathbf{G}}_g\hat{W}_G\end{aligned} \tag{9}$$

where non-dimensional parameters are defined as:

$$\lambda = \frac{\rho_a U_a^2 a^3}{D_s}, \quad \mu_a = \frac{\rho_a a}{\rho_s h_s}, \quad \mu_p = \frac{\rho_p h_p}{\rho_s h_s}, \quad \sigma = \frac{D_p}{D_s}$$

and $\varepsilon = \dfrac{d_{31} V_{\max} a^2 E_p S_p}{D_p h_s (1-\upsilon_p)}$.

3. CONTROL DESIGN

3.1 State space representation

The equation (9) can be written in state space form as

$$\begin{cases} \dot{\mathbf{X}} = \mathbf{A}\mathbf{X} + \mathbf{B}\mathbf{U} + \mathbf{E}\mathbf{V}_g \\ \mathbf{Y} = \mathbf{C}\mathbf{X} \end{cases} \tag{10}$$

for measurable disturbance

$$\dot{\mathbf{V}}_g = \mathbf{A}_0 \mathbf{V}_g \tag{11}$$

Where

$$\mathbf{A} = \begin{bmatrix} \mathbf{0} & \mathbf{I} \\ -(\hat{\mathbf{M}}_s + 4\mu_p \hat{\mathbf{M}}_p)^{-1} \left(\frac{\mu_a}{\lambda}\hat{\mathbf{K}}_s + 4\frac{\mu_a \sigma}{\lambda}\hat{\mathbf{K}}_p + \frac{1}{M_\infty}\hat{\mathbf{L}}\right) & -\frac{1}{4M_\infty}(\hat{\mathbf{M}}_s + 4\mu_p \hat{\mathbf{M}}_p)^{-1}\hat{\mathbf{D}} \end{bmatrix}$$

$$\mathbf{B} = \begin{bmatrix} \mathbf{0} \\ 8\frac{\mu_a \sigma \varepsilon}{\lambda}(\hat{\mathbf{M}}_s + 4\mu_p \hat{\mathbf{M}}_p)^{-1}\hat{\mathbf{\Theta}} \end{bmatrix}$$

$$\mathbf{C}^T = \mathbf{I}$$

$$\mathbf{E} = \begin{bmatrix} \mathbf{0} \\ -\frac{1}{4M_\infty}(\hat{\mathbf{M}}_s + 4\mu_p \hat{\mathbf{M}}_p)^{-1}\hat{\mathbf{G}}_g \end{bmatrix}$$

In this system, the eigenvalues of $\mathbf{A}$ determine the value for λ that clears system stability when $\mathbf{U} = \mathbf{0}$. The flutter boundaries are determined by increasing the non-dimensional dynamic pressure λ while holding all other parameters fixed. Flutter occurs when one of the system eigenvalues moves into the right-half-plane.

3.2 LQR-Integral controller

The optimal flutter control problem must be established as a regulator problem. Through the addition of an integral controller, the system type is increased giving a zero steady state error (Van de Vegte, 1990). Assuming the desired input $\mathbf{Y}_d$ and the disturbance vector $\mathbf{V}_g$ to be constant and stable design with zero steady state error was achieved by using the integral controller. The control would be such that

For: $t \to \infty \Rightarrow \dot{\mathbf{X}} \to 0$ & $\mathbf{Y} \to \mathbf{Y}_d$ (12)

By defining new variable $\boldsymbol{\eta}$ as

$$\boldsymbol{\eta} = \int_0^t (\mathbf{Y} - \mathbf{Y}_d)\, dt \tag{13}$$

And combining it with the equation (10), it can be easily shown that

$$\begin{Bmatrix} \dot{\mathbf{X}} \\ \dot{\boldsymbol{\eta}} \end{Bmatrix} = \begin{bmatrix} \mathbf{A} & \mathbf{0} \\ \mathbf{C} & \mathbf{0} \end{bmatrix} \begin{Bmatrix} \mathbf{X} \\ \boldsymbol{\eta} \end{Bmatrix} + \begin{bmatrix} \mathbf{B} \\ \mathbf{0} \end{bmatrix} \{\mathbf{U}\} + \begin{bmatrix} \mathbf{E} & \mathbf{0} \\ \mathbf{0} & -\mathbf{I} \end{bmatrix} \begin{Bmatrix} \mathbf{V}_g \\ \mathbf{Y}_d \end{Bmatrix} \tag{14}$$

By assuming steady state solutions of the equation (14) as $\mathbf{X}_{ss}$, $\boldsymbol{\eta}_{ss}$ and $\mathbf{U}_{ss}$, it can be shown that new modified state equation now becomes

$$\dot{\mathbf{Z}} = \hat{\mathbf{A}}\mathbf{Z} + \hat{\mathbf{B}}\mathbf{V} \tag{15}$$

Since the desired states for the new variable $\mathbf{Z}$, would be $\mathbf{Z} = \mathbf{0}$, the tracking problem can now be formulated as a regulator. The performance index in terms of the new variable is written as

$$J = \frac{1}{2}\mathbf{Z}^T(t_f)\, N\, \mathbf{Z}(t_f) + \int_0^{t_f} \left(\frac{1}{2}\mathbf{Z}^T(t) Q \mathbf{Z}(t) + \frac{1}{2}\mathbf{V}^T(t) R \mathbf{V}(t)\right) \tag{16}$$

where N, Q and R are weighting matrices and are usually diagonal. Whose solution for a regulator problem results in the control law is

$$\mathbf{V} = \hat{\mathbf{F}}(t)\mathbf{Z}(t), \qquad \hat{\mathbf{F}}(t) = -\mathbf{R}^{-1}\hat{\mathbf{B}}\mathbf{K}(t) \tag{17}$$

where $\mathbf{K}$ is a symmetric and positive definite matrix obtained by solution of the Ricatti equation (Van de Vegte, 1990)

$$\dot{\mathbf{K}} = -\mathbf{K}\hat{\mathbf{A}} - \hat{\mathbf{A}}^T\mathbf{K} + \mathbf{K}\hat{\mathbf{B}}\mathbf{R}^{-1}\hat{\mathbf{B}}^T\mathbf{K} - \mathbf{Q} \tag{18}$$

Therefore the optimal LQR-integral control can be written as

$$\mathbf{U} = -\hat{\mathbf{F}}_1\mathbf{X} - \hat{\mathbf{F}}_2\left[\int_0^{t_f} (\mathbf{Y} - \mathbf{Y}_d)\, dt\right] \tag{19}$$

3.3 Feedforward controller for measurable disturbance

While with integral control the static errors can be made zero, the errors during the transients may be large. Feedforward control is an important technique in practice to reduce the effect of disturbances if these are measurable (Van de Vegte, 1990). Using the assumption of constant steady state values $\mathbf{Y}_d$ and disturbance vector $\mathbf{V}_g$, the system and the output equations are written as follows

$$\begin{Bmatrix} \dot{\mathbf{X}} \\ \mathbf{Y} - \mathbf{Y}_d \end{Bmatrix} = \mathbf{G}\begin{Bmatrix} \mathbf{X} \\ \mathbf{U} \end{Bmatrix} + \mathbf{H}\begin{Bmatrix} \mathbf{V}_g \\ \mathbf{Y}_d \end{Bmatrix} \tag{20}$$

where

$$\mathbf{G}=\begin{bmatrix}\mathbf{A} & \mathbf{B}\\ \mathbf{C} & \mathbf{0}\end{bmatrix},\qquad \mathbf{H}=\begin{bmatrix}\mathbf{E} & \mathbf{0}\\ \mathbf{0} & -\mathbf{I}\end{bmatrix} \tag{21}$$

The purpose of the controller is to satisfy the conditions in equation (12), with the disturbances present. For the steady state part of the solution the stable form of $\mathbf{X}_{ss}$ and $\mathbf{U}_{ss}$ must satisfy, and implementing this result would again yield a regular problem with the control law

$$\mathbf{U}=-\hat{\mathbf{F}}\,\mathbf{X}+\begin{bmatrix}\hat{\mathbf{F}} & \mathbf{I}\end{bmatrix}\mathbf{G}^{-1}\,\mathbf{H}\begin{Bmatrix}\mathbf{V}_g\\ \mathbf{Y}_d\end{Bmatrix} \tag{22}$$

Which clearly shows that the controller is proportional to the states feedback and also to the feedforward of $\mathbf{V}_g$ and $\mathbf{Y}_d$.

3.4 Feedforward plus LQR-Integral controller

The final control law is an optimal LQR incorporated in addition to integrator and feedforward controllers

$$\mathbf{U}=-\hat{\mathbf{F}}_1\mathbf{X}-\hat{\mathbf{F}}_2\left(\int_0^{t_f}(\mathbf{Y}-\mathbf{Y}_d)\,dt\right)-\hat{\mathbf{F}}_3\begin{Bmatrix}\mathbf{V}_g\\ \mathbf{Y}_d\end{Bmatrix} \tag{23}$$

where

$$\hat{\mathbf{F}}_3=[\,\hat{\mathbf{F}}_1\quad\mathbf{I}\,]\mathbf{G}^{-1}\,\mathbf{H} \tag{24}$$

As evident by equation (23), there are three terms in the control law. The first is the feedback of the states (LQR); the second term is related to the integral control (Int). The third term is a feedforward (FF) of the disturbance and the desired input vector. figure 3 shows the final design in block diagram form.

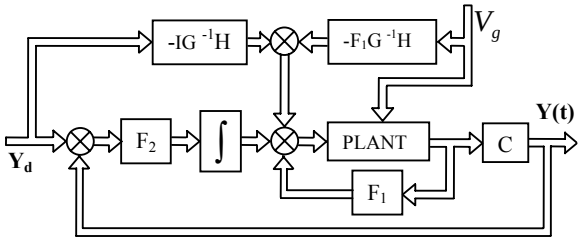

Figure 3: *Proposed system in block diagram.*

4. RESULTS AND DISCUSSION

The numerical simulation is based on a rectangular panel and all four edges are simply supported. The non-dimensional parameters of the panel are $\mu_a=0.1$, $\mu_p=0.5$, $\sigma=1.5$, $\varepsilon=100$ and $a/b=1$.

These parameters correspond to typical values for G-1195-type piezoelectric, steel panel and sea level air conditions. According to , the results are represented by four linear modes ($N=4$) in equation (7).

Analysis of results is done in two general states: existence of gust ($\mathbf{V}_g\neq 0$) and not existence of gust ($\mathbf{V}_g=\mathbf{0}$). In absent gust, at first the accuracy of method and equations is compared to (Frampton et al, 1996), and then flutter dynamic pressure is calculated for each of three arrangements of piezoelectric placement and their dimensions through LQR method. In the state of existence of gust, undesirable panel responses are controlled by using LQR incorporated in addition to integrator (Int) and feedforward (FF) controllers for zero desired output ($\mathbf{Y}_d=\mathbf{0}$).

Before proceeding to flutter suppression analysis of the panel, the flutter boundaries of simply supported edge isotropic panel is solved by the same parameters: $\mu_a=0.1$, $\mu_p=0.5$, $\sigma=1.2$, $\varepsilon=130$, $a/b=1$, $\bar{x}=0.7a$, $\Delta x=0.2a$, $y_1=0.4b$ and $y_2=0.6b$ as test examples to validate the present formulation and solution method. The results of non-dimensional flutter dynamic pressure vs Mach number without gust effects are validated with results of (Frampton et al, 1996) and excellent agreement is observed, as figure 4.

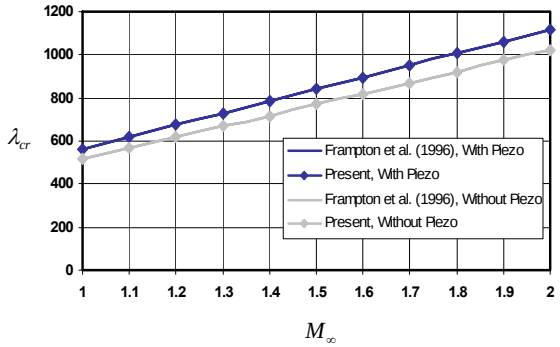

Figure 4: *Non-dimensional dynamic pressure vs Mach number for a square panel.*

4.1 Configuration study

The results of passive and active LQR flutter control methods for two configurations of piezo actuators are analyzed in this part by calling square and cross configurations as shown in figure 5. The results in this study is for install location of a piezo actuators at $\hat{x}=0.25a,0.5a,0.75a$, $\Delta x=0.1a$, and $\Delta y=0.1b$.

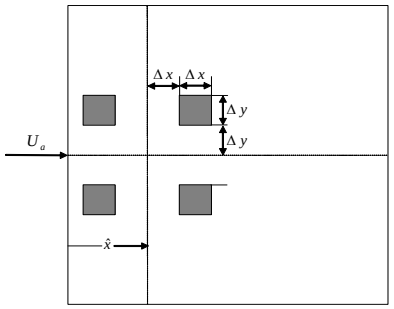

(a)

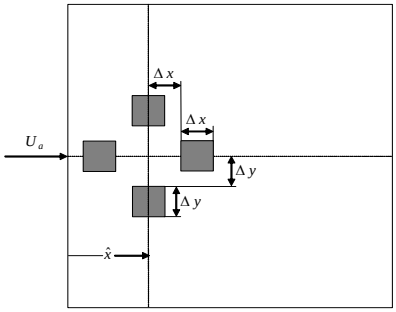

(b)

Figure 5: *Piezo segments configurations: (a) square configuration, (b) cross configuration.*

Critical dynamic pressure results for two different segment configurations are showed in tables 1 and 2. "Base panel" means non-dimensional flutter dynamic pressure of the panel with no piezo actuators, "passive control" is referred to flutter dynamic pressure of the panel with no voltage, "Active control" is related to flutter dynamic pressure with maximum voltage of the piezo actuators and "λ_{cr} Increase" is the ratio of the "Active control" to "Base panel".

	$\hat{x}$		
	0.25a	*0.5a*	*0.75a*
Base Panel	1022	1022	1022
Passive Control	1131	1141	1125
Active Control	1988	2032	1940
λ_{cr} **Increase**	0.94	0.98	0.89

Table 1: Square configuration at $M_\infty = 2$.

	$\hat{x}$		
	0.25a	*0.5a*	*0.75a*
Base Panel	1022	1022	1022
Passive Control	1143	1138	1155
Active Control	2037	1990	2095
λ_{cr} **Increase**	0.99	0.94	1.05

Table 2: Cross configuration at $M_\infty = 2$.

4.2 Investigation of controller capability

In this section by utilizing all three controllers, effects of gust on panel deflection are discussed. According to previous section 5.2 two best configuration of piezo actuators are selected. Panel deflection time histories at point $\bar{x} = 0.75a$ and $\bar{y} = 0.5b$ are shown in figures 6 and 7. In figure 6a, it can be seen flutter response for open loop for square configuration at $\hat{x} = 0.5a$. Alleviation of gust responses is shown in figure 6b for three controllers design. As illustrated, the best state of flutter suppression and gust alleviation are achieved by utilizing LQR incorporated in addition to integrator (Int) and feedforward (FF) controllers. As shown in figure 6b integrator controller helps to reach zero steady state error and feedforward controller efforts to improve transient response. The same study is done for cross configuration at $\hat{x} = 0.75a$. In figures 7a and 7b results of both open loop and closed loop of cross shape of piezo actuators are shown respectively. In this analysis best results are relate to applying all three controllers (LQR + Int + FF).

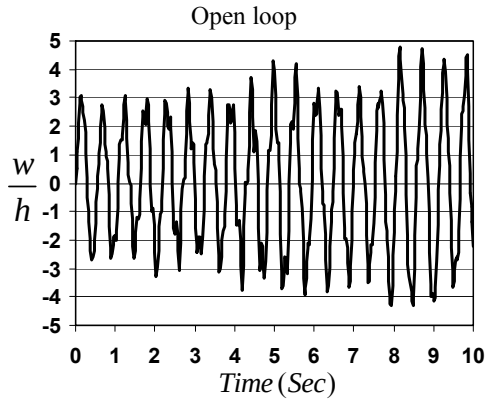

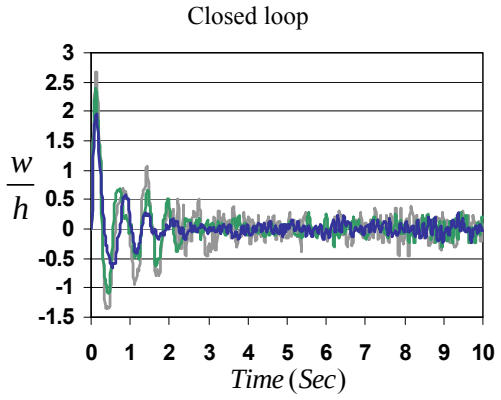

Figure 6: *Time history with gust effects at* $M_\infty = 2$, $\hat{x} = 0.5a$ *&* $\lambda = 1150$ *for square configuration:*

open loop, LQR, LQR + Int, LQR + Int + FF.

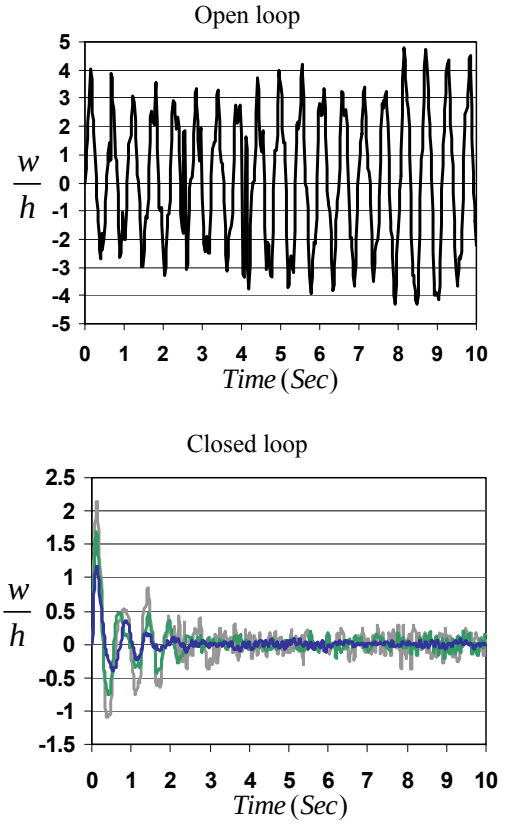

Figure 7: *Time history with gust effects at* $M_\infty = 2$ $\hat{x} = 0.75a$ & $\lambda = 1165$ *for cross configuration:*

open loop, LQR, LQR + Int, LQR + Int + FF.

5. CONCLUSIONS

In this study, an investigation on the feasibility of employing segmented piezoelectric actuators to suppress panel flutter and gust response of a rectangular panel has been presented. For a piece of information both the piezo actuator placements and their configurations affects on panel flutter conditions, are studied for two configurations of piezoelectric actuator. It was shown that this type of model is capable of significantly increasing the non-dimensional flutter dynamic pressure. Furthermore an optimal feedforward/integral control for piezoelectric panel flutter suppression and gust alleviation is developed. Optimal controllers are designed, successfully controlled the panel flutter and the gust responses for various piezo configurations.

6. REFERENCES

Alkhatib, R., Golnaraghi, M. F.,2003, Active structural vibration control: a review. *The Shock and Vibration Digest*, **35**: 367–383.

Baily, J., Habbard, J. E., 1985, Distributed piezoelectric-polymer active vibration control of a cantilever beam. *Journal of Guidance, Control and Dynamic*, **8**: 605-611.

Chopra, 2002, Review of state of art of smart structures and integrated systems. *AIAA Journal*, **40**: 2145–2187.

Frampton, K. D. et al, 1996, Active control of panel flutter with piezoelectric transducers. *Journal of Aircraft*, **33**: 768-774.

Hagood, N. W. et al, 1990, Modelling of piezoelectric actuator dynamics for active structural control. *Journal of Intelligent Material Systems and Structures*, **1**: 327-354.

Han, J. H. et al, 2006, Active flutter suppression of a lifting surface using piezoelectric actuation and modern control. *Journal of Sound and Vibration*, **291**: 706–722.

Ghanbarpoor asl, H. et al, 2004, Smart cantilevered supersonic panel with LQG control under random gust excitation. *Second International Conference of Iranian Aerospace Society, Aerspace2004*, 209-219, Isfahan, Iran.

Moon, S.H., Kim, S.J., 2003, Suppression of nonlinear composite panel flutter with active/passive hybrid piezoelectric networks using finite element method. *Composite Structures*, **59**: 525–533.

Sadri, A. M. et al, 2002, LQG control design for panel flutter suppression using piezoelectric actuators. *Smart Materials and Structures*, **11**: 834-839.

Scott, R. C., Weisshaar, T. A., 1994, Panel flutter suppression using adaptive material actuators. *Journal of Aircraft*, **31**: 213-222.

Sebastijanovic, N. et al, 2007, Panel flutter detection and control using the eigenvector orientation method and piezoelectric layers. *AIAA Journal*, **45**: 118-127.

Van de Vegte, J., 1990, Feedback Control System. Englewood Cliffs, Prentice-Hall.